© 2016. Published by The Company of Biologists Ltd | Journal of Cell Science (2016) 129, 1018-1030 doi:10.1242/jcs.176883

RESEARCH ARTICLE

Pannexin 3 and connexin 43 modulate skeletal development through their distinct functions and expression patterns

Masaki Ishikawa[1,2], Geneva L. Williams[1,3], Tomoko Ikeuchi[1], Kiyoshi Sakai[1,4], Satoshi Fukumoto[5] and Yoshihiko Yamada[1,*]

ABSTRACT

Pannexin 3 (Panx3) and connexin 43 (Cx43; also known as GJA1) are two major gap junction proteins expressed in osteoblasts. Here, we studied their functional relationships in skeletal formation by generating *Panx3*$^{-/-}$ and *Panx3*$^{-/-}$;*Cx43*$^{-/-}$ mice and comparing their skeletal phenotypes with *Cx43*$^{-/-}$ mice. *Panx3*$^{-/-}$ mice displayed defects in endochondral and intramembranous ossification, resulting in severe dwarfism and reduced bone density. The skeletal abnormalities of *Panx3*$^{-/-}$;*Cx43*$^{-/-}$ mice were similar to those in *Panx3*$^{-/-}$ mice. The gross appearance of newborn *Cx43*$^{-/-}$ skeletons showed no obvious abnormalities, except for less mineralization of the skull. In *Panx3*$^{-/-}$ mice, proliferation of chondrocytes and osteoblasts increased and differentiation of these cells was inhibited. Panx3 promoted expression of osteogenic proteins such as ALP and Ocn (also known as ALPL and BGLAP, respectively), as well as Cx43, by regulating Osx (also known as SP7) expression. Panx3 was induced in the early differentiation stage and reduced during the maturation stage of osteoblasts, when Cx43 expression increased in order to promote mineralization. Furthermore, only Panx3 functioned as an endoplasmic reticulum (ER) Ca^{2+} channel to promote differentiation, and it could rescue mineralization defects in *Cx43*$^{-/-}$ calvarial cells. Our findings reveal that Panx3 and Cx43 have distinct functions in skeletal formation.

KEY WORDS: Pannexin 3, Connexin 43, Skeletal formation, Ossification, Chondrocyte, Osteoblast

INTRODUCTION

Cell–cell and cell–matrix communication regulates the activation of signaling pathways involved in cell functioning, proliferation, differentiation and death. Gap junction proteins play important roles in such cellular communication (Giepmans, 2004; Hervé and Derangeon, 2013). There are two gap junction families in vertebrates: the connexins (Cxs), containing more than 20 members (Söhl and Willecke, 2004), and the recently identified pannexins (Panxs) (Baranova et al., 2004). The Panx family consists of three members, Panx1, Panx2 and Panx3 (D'Hondt et al., 2009; Söhl and Willecke, 2004). Gap junction proteins form hexamers to create channels, which can exchange small molecules, such as ions and inositol (1,4,5)-trisphosphate (IP_3), between neighboring cells and from the cell to the extracellular space (through gap junctions and hemichannels, respectively) (Barbe et al., 2006; D'Hondt et al., 2009; Söhl and Willecke, 2004). Panxs can also function as an endoplasmic reticulum (ER) Ca^{2+} channel, propagating intracellular Ca^{2+} from the ER and increasing intracellular Ca^{2+} levels (Ishikawa et al., 2011; Vanden Abeele et al., 2006).

Bone development is a highly coordinated process (Rodda and McMahon, 2006). Bones are formed through two mechanisms: endochondral ossification and intramembranous ossification. Endochondral ossification, observed in most of the long bones, involves the formation of cartilage as a template initiated by mesenchymal cell condensation. Mesenchymal cells in the condensed area differentiate into chondrocytes, which proliferate and then further differentiate into mature hypertrophic chondrocytes, which later are replaced by bone cells. Mesenchymal cells at the periphery of the condensation give rise to the perichondrium, which differentiates into osteoblasts and forms a bone collar (Karsenty and Wagner, 2002; Kronenberg, 2003; Zelzer et al., 2002). Bones that are not formed through the endochondral process, such as the skull and maxillomandibular bones, are formed by intramembranous ossification. In this process, mesenchymal cells directly differentiate into osteoblasts and deposit bone matrix proteins (Lustig et al., 2002).

Among the members of the Cx family, Cx43 (also known as GJA1) is the most abundantly expressed in osteoblastic cells (Civitelli, 2008). Cx43 mutations cause syndactyly, enamel hypoplasia, and oculodentodigital dysplasia (ODDD) (Paznekas et al., 2003; Watkins et al., 2011). Cx43-null (*Cx43*$^{-/-}$) mice die soon after birth due to cardiovascular malformation (Reaume et al., 1995) and show less bone mineralization, especially in calvarial bone (Lecanda et al., 2000). Mice with a conditional knockout of *Cx43* specific to skeletal tissues show delayed bone formation and reduced mineralization in calvarial and cortical bones (Chung et al., 2006; Plotkin et al., 2008; Watkins et al., 2011).

Panx3 is highly expressed in hard tissues, such as cartilage and bone (Iwamoto et al., 2010; Ishikawa, 2011). Using cell culture, we have previously shown that Panx3 promotes chondrocyte differentiation by regulating intracellular ATP and cAMP levels through a Panx3 hemichannel, which in turn counteracts the parathyroid hormone (PTH)–PTHrP signaling pathway (Iwamoto et al., 2010). We also demonstrated that Panx3 functions as a hemichannel, an ER Ca^{2+} channel and a gap junction, and that it promotes osteoblast differentiation (Ishikawa et al., 2011). In addition, Panx3 promotes osteoprogenitor cell cycle exit by inhibiting Wnt/β-catenin signaling through its action as a hemichannel (Ishikawa et al., 2014).

In this study, we generated *Panx3*-null (*Panx3*$^{-/-}$) mice and *Panx3* and *Cx43* double-null (*Panx3*$^{-/-}$;*Cx43*$^{-/-}$) mice, to identify the distinct functional relationships of Panx3 and Cx43 in skeletal

[1]Laboratory of Cell and Developmental Biology, National Institute of Dental and Craniofacial Research, National Institutes of Health, Bethesda, MD 20814, USA. [2]Operative Dentistry, Tohoku University Graduate School of Dentistry, Sendai 980-8575, Japan. [3]Division of Biology & Biomedical Sciences, Washington University in St. Louis, St. Louis, MO 63110, USA. [4]Department of Oral and Maxillofacial Surgery, Nagoya University Graduate School of Medicine, Nagoya 466-8550, Japan. [5]Department of Pediatric Dentistry, Tohoku University Graduate School of Dentistry, Sendai 980-8576, Japan.

*Author for correspondence (yoshi.yamada@nih.gov)

Received 20 July 2015; Accepted 5 January 2016

Journal of Cell Science (2016) 129, 1018-1030 doi:10.1242/jcs.176883

formation, and compared their skeletal phenotypes with Cx43-null (*Cx43*$^{-/-}$) mice. *Panx3*$^{-/-}$ mice showed reduced bone density and marked dwarfism caused by defects in both endochondral and intramembranous ossification. We show that Panx3 regulates differentiation of mature hypertrophic chondrocytes, which express vascular endothelial growth factor (VEGF), which is essential for vascular invasion into cartilage and endochondral ossification. Panx3 also plays a role in osteogenesis by modulating Wnt/β-catenin signaling and inducing osterix (Osx; also known as SP7) for subsequent differentiation, whereas Cx43 plays a role in the maturation stage. Panx3 is able to substitute for Cx43, whereas Cx43 is not able is able to substitute for Panx3. We demonstrate that this difference is primarily because Cx43 lacks ER Ca^{2+} channel function. Our *in vivo* results demonstrate that Panx3 and Cx43 play distinct functions in skeletal development.

RESULTS

Panx3-null mice display skeletal abnormalities

To study the role of Panx3 in skeletal development, *Panx3*$^{-/-}$ mice were created (Fig. S1A; Table S2). Although the *Panx3*$^{-/-}$ mice survived, they displayed significantly smaller body sizes than the control group of wild-type (WT) mice at birth and throughout adult life (data not shown). Skeletal staining of newborn *Panx3*$^{-/-}$ mice with Alizarin Red (bone) and Alcian Blue (cartilage) showed that the appendicular and axial bones, such as the limbs, skull, clavicles, spines and ribs, were shorter than those of WT mice (Fig. 1A). Dorsal, ventral and lateral views of the skulls showed that all of the skull bones of *Panx3*$^{-/-}$ mice, such as the frontal, parietal, basisphenoid, mandibular and maxilla bones, were smaller than those of WT mice (Fig. 1Ba–c). Mineralization defects were also observed in *Panx3*$^{-/-}$ cranial vaults.

Increased proliferative and prehypertrophic zones and a reduced hypertrophic zone in the *Panx3*-null growth plate

Histology and gene expression analysis were used to examine defects in chondrocyte differentiation in the tibia growth plate of newborn *Panx3*$^{-/-}$ mice. *Panx3*$^{-/-}$ mice showed shortened hindlimbs and forelimbs as compared to WT mice (Fig. 2A). Using hematoxylin and eosin (H&E) staining, it was evident that the proliferative and prehypertrophic zones of *Panx3*$^{-/-}$ mice were elongated, whereas the hypertrophic zone was reduced (Fig. 2Ba,b). Quantitative real-time PCR (qPCR) analyses using mRNA from whole tibias also supported these findings (Fig. 2C). The levels of mRNA for proliferative chondrocyte markers collagen II (*Col2a1*) and aggrecan (*Agc1*, also known as *Acan*), as well as those for prehypertrophic chondrocyte marker *Ihh*, were increased in *Panx3*$^{-/-}$ tibias. *In situ* hybridization revealed an increase in Ihh-positive cells and expansion of the prehypertrophic zone in Panx3$^{-/-}$ growth plates (Fig. S1B). However, the expression level of collagen type X (*Col10a1*), a marker of prehypertrophic and hypertrophic chondrocytes, was similar in the WT and *Panx3*$^{-/-}$ tibias (Fig. 2C).

Differentiation of mature hypertrophic chondrocytes is inhibited in the *Panx3*-null growth plate

Hypertrophic chondrocytes differentiate into mature hypertrophic chondrocytes to form a few cell layers at the end of the growth plate adjacent to the chondro-osseous junction. The matrix surrounding terminally differentiated mature hypertrophic chondrocytes becomes mineralized, and the chondrocytes are replaced with osteoblasts to form trabecular bone. During cartilage replacement, the cartilage matrix and mineralized tissues must be removed; matrix metalloproteinase 13 (MMP13) and VEGF, produced by the mature hypertrophic chondrocytes, are required for this process (Kronenberg, 2003). Immunostaining analysis showed that the expression of VEGF, MMP13 and osteopontin (OPN, also known as SPP1) was reduced in the growth plates of *Panx3*$^{-/-}$ mice relative to WT control, indicating that mature chondrocyte differentiation was inhibited in the *Panx3*$^{-/-}$ growth plate (Fig. 3A). VEGF, expressed by the mature chondrocytes, is required for vascular invasion in the chondro-osseous boundary (Zelzer et al., 2002). Staining for the

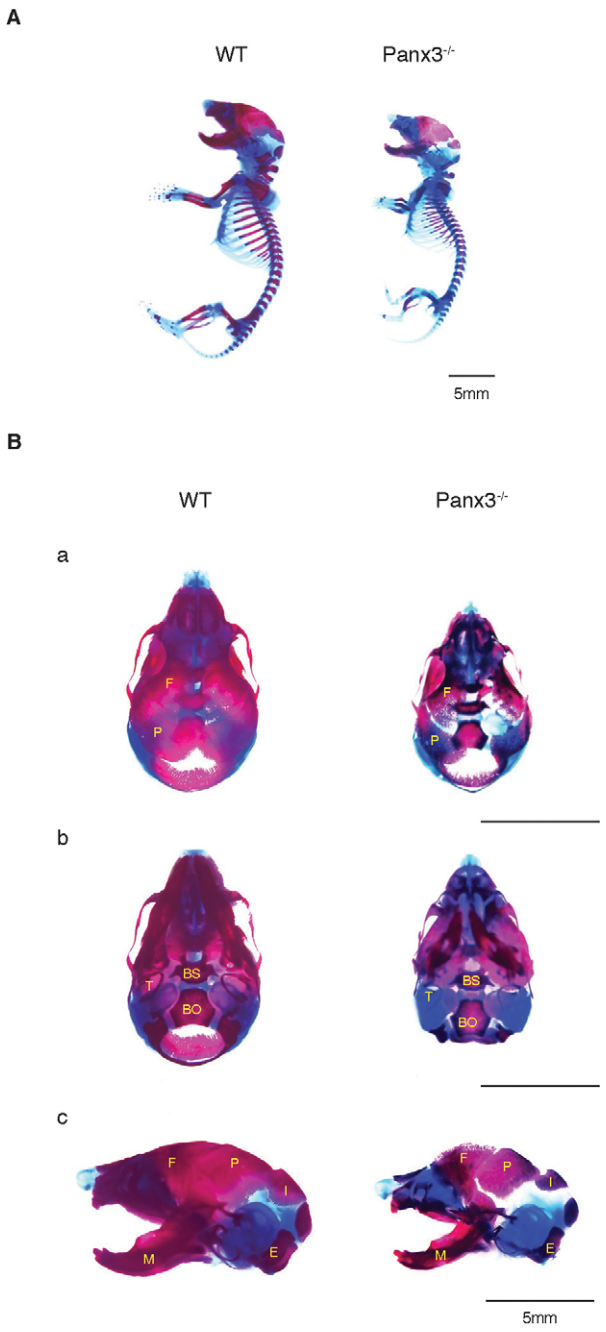

Fig. 1. Skeletal abnormalities of newborn *Panx3*-null mice. (A) Whole-body skeletal staining of newborn WT and *Panx3*$^{-/-}$ mice with Alizarin Red for bone and Alcian Blue for cartilage. (B) Defects in skull development in newborn *Panx3*$^{-/-}$ mice. (a) Dorsal, (b) ventral and (c) lateral views of the Alizarin Red and Alcian Blue staining in skulls of WT (left lane) and *Panx3*$^{-/-}$ (right lane) mice. F, frontal bone; P, parietal bone; T, tympanic ring; BS, basisphenoid bone; BO, basioccipital bone; I, interparietal bone; E, exoccipital bone; M, mandibular.

Journal of Cell Science (2016) 129, 1018-1030 doi:10.1242/jcs.176883

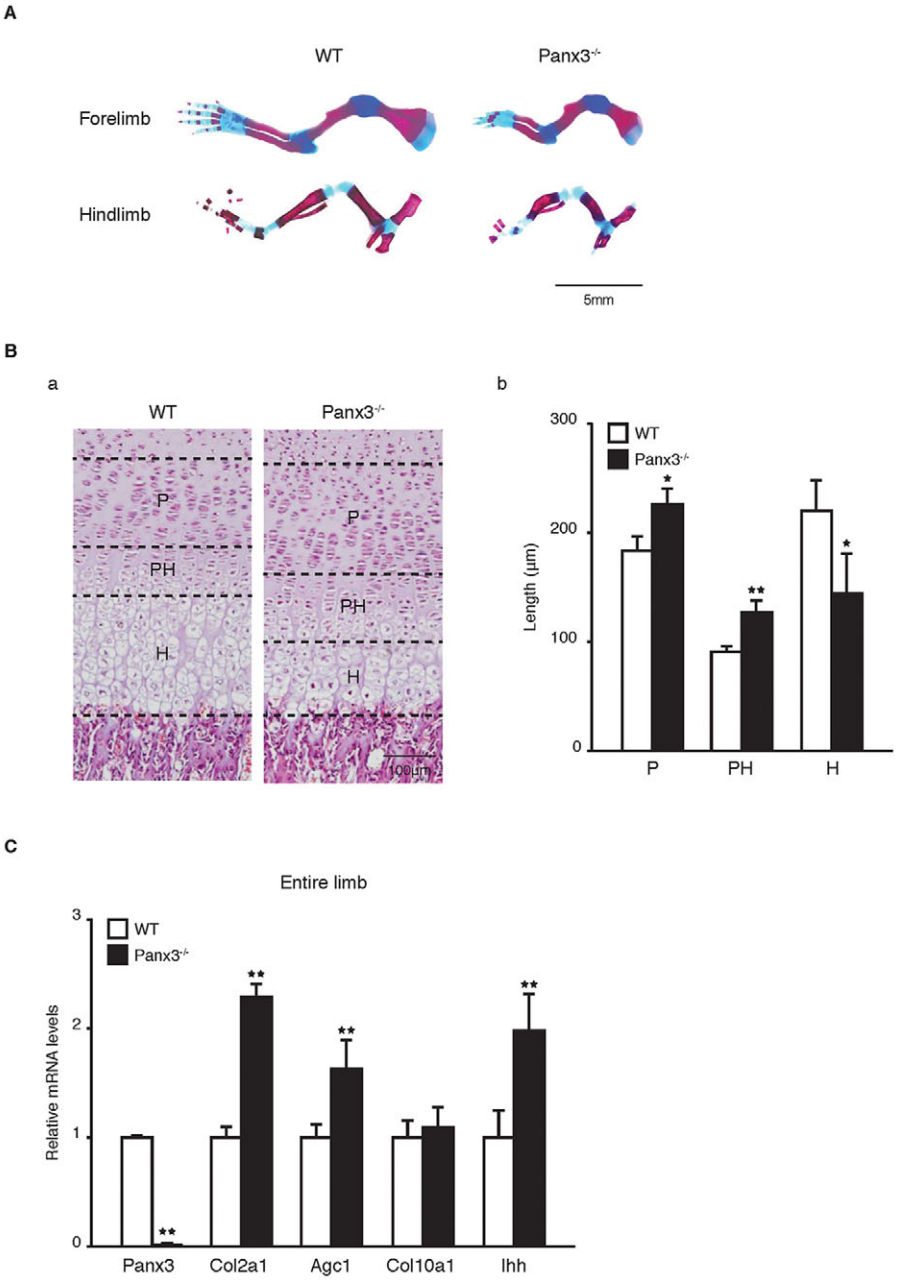

Fig. 2. Expanded proliferative and prehypertrophic zones, but a smaller hypertrophic zone, in *Panx3*-null mice. (A) The forelimbs and hindlimbs of newborn WT and *Panx3*$^{-/-}$ mice stained with Alizarin Red and Alcian Blue. (B) Histology for growth plate of newborn mice. (a) H&E staining. (b) Quantifications of the lengths in each zone in cartilage areas. P, proliferative zone; PH, prehypertrophic zone; H, hypertrophic zone. (C) qPCR for mRNA expression of the chondrocyte marker genes using total RNA isolated from whole tibias. **P*<0.05; ***P*<0.01 (Student's *t*-tests). Results represent mean±s.d. of three independent experiments.

endothelial cell marker CD31 (also known as PECAM1) was reduced in the *Panx3*$^{-/-}$ growth plate (Fig. 3Ba). Furthermore, development of secondary ossification center was delayed in *Panx3*$^{-/-}$ mice at postnatal day (P)10 (Fig. S2A), indicating reduced vascular invasion. In WT mice, TRAP-positive differentiated osteoclasts migrated into the boundary through the vasculature in the growth plate. However, the number of TRAP-positive osteoclasts was reduced in *Panx3*$^{-/-}$ growth plates (Fig. 3Bb). When bone marrow stromal cells (BMSCs) from WT mice were induced to differentiate into osteoclasts, there was little induction of Panx3 expression, whereas Cx43 expression was induced (Fig. S3Ba,b). There was no significant difference in the amount of osteoclast differentiation induced by RANKL (also known as TNFSF11) with macrophage colony-stimulating factor (M-CSF) between osteoclast progenitor cells from WT and Panx3$^{-/-}$ bone marrow (data not shown), suggesting the indirect involvement of Panx3 in osteoclast differentiation. Given that osteoblasts regulate osteoclast differentiation through RANKL and OPG (also known as TNFRSF11B), we examined the involvement of osteoblast progenitors in osteoclast differentiation using co-cultures of osteoblast progenitors and osteoclast progenitors from both WT and *Panx3*$^{-/-}$ calvaria. In co-cultures of primary calvarial cells enriched in both osteoblast progenitors and osteoclast progenitors isolated from the P1 *Panx3*$^{-/-}$ mice, the levels of osteoclast differentiation was reduced in the cells from *Panx3*$^{-/-}$ calvaria, compared with that of WT calvaria (Fig. S3C). These results indicate that Panx3 regulates osteoclast differentiation through Panx3-mediated osteoblast differentiation.

Osteoblast and osteoclast differentiation is inhibited in the *Panx3*-null growth plate

We next examined bone formation and the differentiation of osteoblasts and osteoclasts in *Panx3*$^{-/-}$ tibias and calvaria (Fig. 4; Figs S2B and S3). Von Kossa staining revealed that the formation of

Journal of Cell Science (2016) 129, 1018-1030 doi:10.1242/jcs.176883

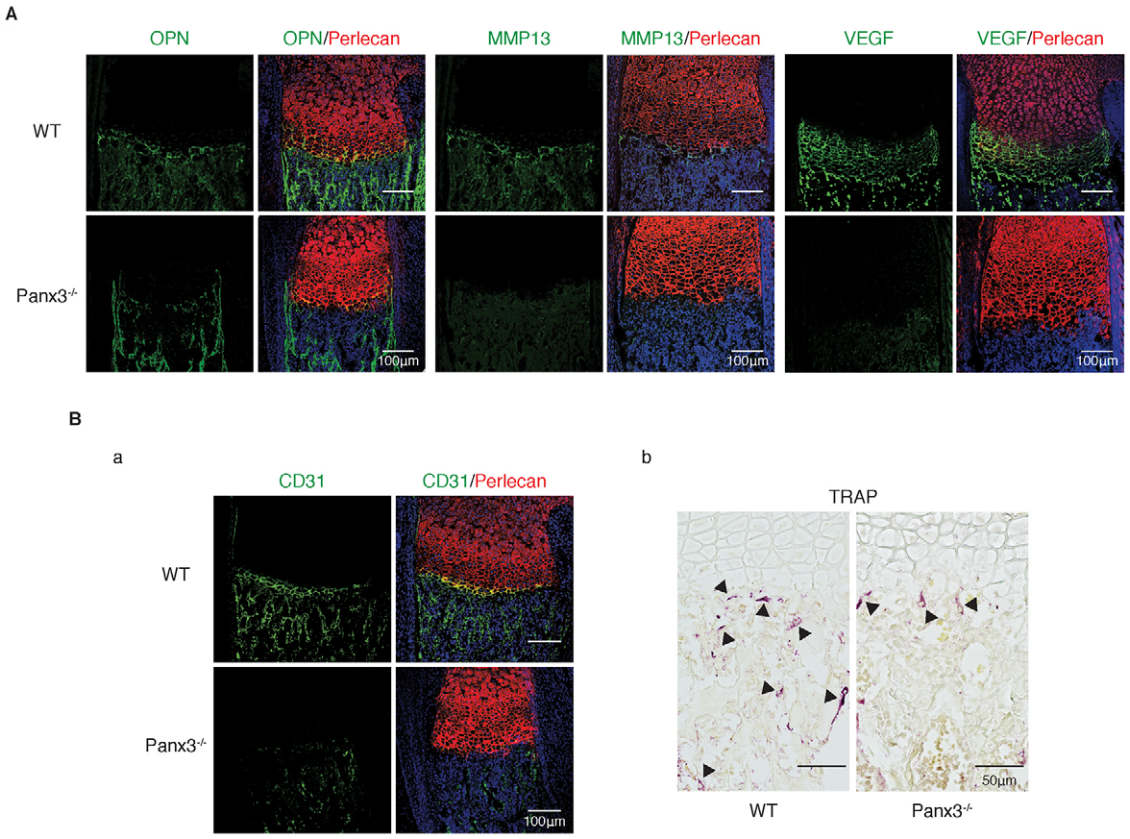

Fig. 3. *Panx3* knockout inhibits chondrocyte terminal differentiation. (A) Immunostaining of the growth plate of newborn WT and *Panx3*$^{-/-}$ tibias with antibodies to OPN (green), MMP13 (green) or VEGF (green). (B) CD31 (green) staining (a) and TRAP staining (b) of the growth plate of WT and *Panx3*$^{-/-}$ tibias. Perlecan (red) staining shows cartilage areas; nuclei were stained with Hoechst dye 33342 (blue in A and Ba).

the bone collar and the trabecular bone was reduced in the *Panx3*$^{-/-}$ tibias (Fig. 4Aa). Bone collar formation was visualized by double staining with calcein (performing two different calcein injections in the tibia: the first injection at P10 and the second injection at P17, with imaging conducted at P18). The staining showed that bone collar formation in *Panx3*$^{-/-}$ tibias was less than that of WT tibias (Fig. 4Ab). Immunostaining of newborn tibias showed that osteoblast markers Osx and alkaline phosphatase (ALP, also known as ALPL) were expressed in the periosteum, bone collar, and trabecular bone of WT growth plates; whereas the same areas of *Panx3*$^{-/-}$ tibias displayed decreased expression of these markers (Fig. 4B). The reduced expression of Osx and ALP proteins was also confirmed at the mRNA level by qPCR analysis, using mRNA prepared from whole tibias (Fig. 4C). The mRNA levels of the mature osteoblast differentiation marker *Ocn* (also known as *Bglap*) were also reduced in *Panx3*$^{-/-}$ mice; whereas the expression levels of *Runx2*, a master transcription factor for osteoblast differentiation, were similar between *Panx3*$^{-/-}$ and WT tibias (Fig. 4C). Expression levels of the osteocyte markers dentin matrix protein 1 (*Dmp1*) and sclerostin (*Sost*) were also reduced in *Panx3*$^{-/-}$ tibias (Fig. 4C). We also confirmed the Panx3-mediated *Osx* regulation by generating *Panx3*$^{-/-}$;*Osx-GFP* mice and tracing the endogenous *Osx* expression. The number of Osx–GFP-positive cells was reduced in *Panx3*$^{-/-}$ tibias (Fig. 4D).

An increase in the intracellular Ca^{2+} level ($[Ca2^{+}]_i$) activates the phosphatase calcineurin and the transcription factor NFATc1 through calmodulin (CaM) signaling, which promotes osteoblast differentiation and bone formation (Berridge et al., 2000; Seo et al., 2009; Zayzafoon, 2006). Inactive phosphorylated NFATc1 is activated through dephosphorylation by calcineurin and can promote expression of osteoblast genes (Koga et al., 2005; Nakashima et al., 2002). Therefore, we examined the phosphorylation levels of Ca^{2+}/CaM-dependent protein kinase II (CaMKII) and NFATc1 in WT and *Panx3*$^{-/-}$ calvarial cells (Fig. 4E). The phosphorylation level of CaMKII was reduced in *Panx3*$^{-/-}$ calvairal cells, indicating reduced CaM signaling. The level of inactive phosphorylated NFATc1 was higher in the *Panx3*$^{-/-}$ cells compared with WT cells. Active Akt is necessary for activation of the Panx3 ER Ca^{2+} channel to increase the release of $[Ca^{2+}]_i$ from the ER (Ishikawa et al., 2011). The levels of active phosphorylated Akt level were reduced in the *Panx3*$^{-/-}$ cells (Fig. 4E). These results suggest that reduced Akt–CaM–NFATc1 signaling causes the decrease in expression of osteoblast marker genes, which is consistent with our previous cell culture study (Ishikawa et al., 2011).

Furthermore, the mRNA expression levels of osteoclast differentiation markers, such as calcitonin receptor (*Ctr*, also known as *Calcr*), matrix metalloproteinase-9 (*Mmp9*), cathepsin K (*CtsK*) and *TRAP* (also known as *Acp5*), were decreased in *Panx3*$^{-/-}$ tibias (Fig. S4). TRAP staining in *Panx3*$^{-/-}$ calvaria was also reduced (Fig. S3A). These results indicate that Panx3 deficiency reduced the differentiation of osteoblasts and osteoclasts.

Proliferation of chondrocytes and osteoblast progenitors is increased in the *Panx3*-null tibia and calvaria

We examined the proliferation of chondrocytes and osteoblast progenitors in the tibia and calvaria of *Panx3*$^{-/-}$ mice (Fig. 5). Fig. 5A illustrates immunostaining for Ki67, a marker of

Journal of Cell Science (2016) 129, 1018-1030 doi:10.1242/jcs.176883

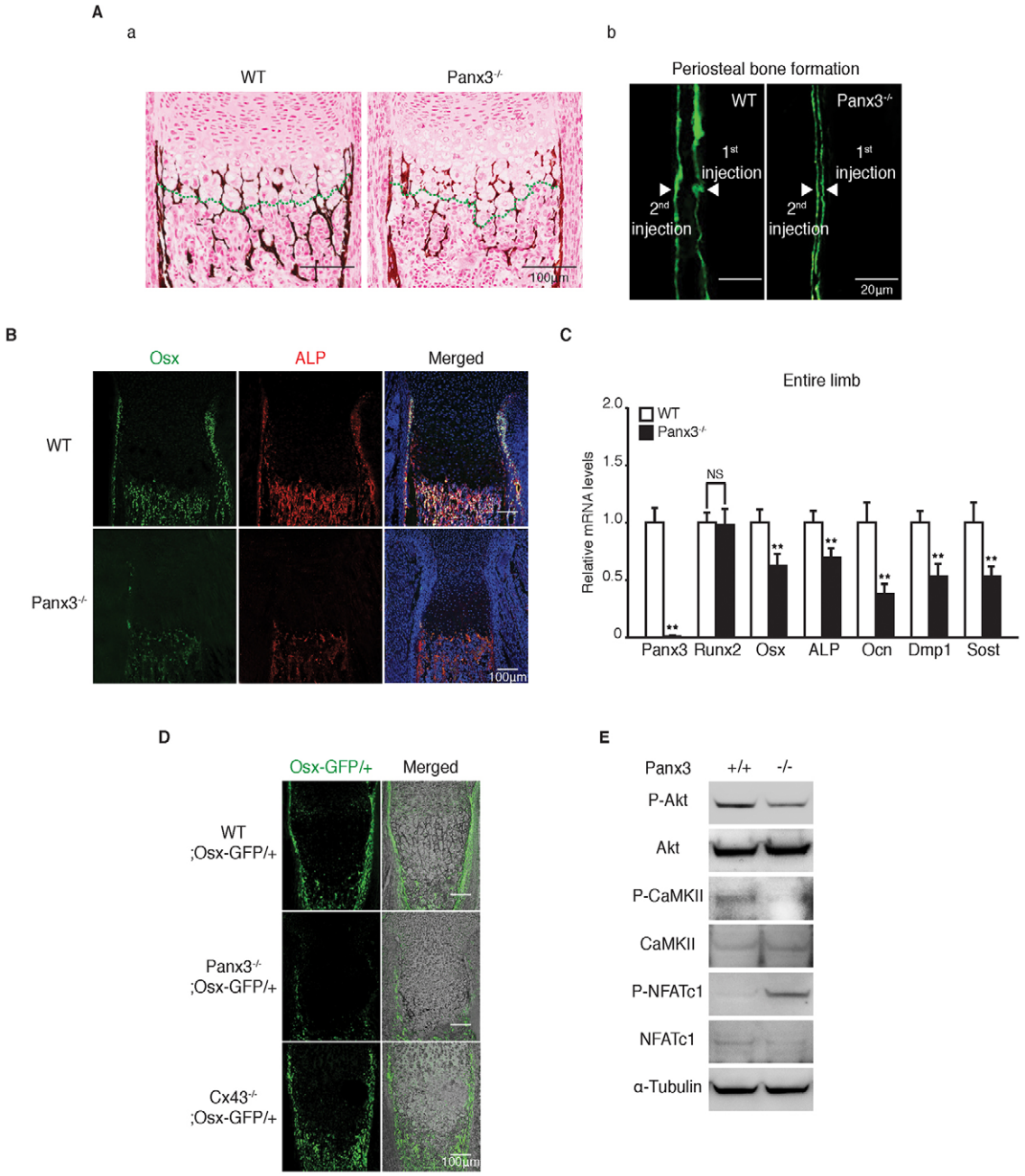

Fig. 4. *Panx3* knockout inhibits osteoblast differentiation. (A) (a) Double staining of Safranin-O (red) and von Kossa (brown) of the growth plates of tibias in newborn WT and *Panx3*$^{-/-}$ mice. (b) New bone formation was analyzed by double calcein labeling [injecting calcein at P10 (1st injection) and at P17 (2nd injection)]. Samples were collected at P18. The spacing of the calcein-labeled layers between the 1st injection and the 2nd injection, shown by arrowheads, represents the bone formed between the injection times. (B) Immunostaining of the growth plates in tibias of newborn WT and *Panx3*$^{-/-}$ mice for Osx (green) and ALP (red). The nuclei were stained with Hoechst 33342 (blue). (C) qPCR for Panx3, osteoblast markers (*Runx2*, *Osx*, *ALP* and *Ocn*) and osteocyte markers (*Dmp1* and *Sost*) using total RNA prepared from whole tibias of newborn mice. Results represent the mean±s.d., n=3. **P<0.01. NS, not significant (Student's t-tests). (D) Osx–GFP expression in *Panx3*$^{-/-}$ and *Cx43*$^{-/-}$ growth plates. The Osx–GFP expression is reduced in the *Panx3*$^{-/-}$ growth plate but not the *Cx43*$^{-/-}$ growth plate. Osx–GFP expression of the growth plates in the tibias of newborn WT *Osx-GFP*/+ mice, *Panx3*$^{-/-}$;*Osx-GFP*/+ mice, and *Cx43*$^{-/-}$; *Osx-GFP*/+ mice. The right panels show merged images of GFP (green) and light microscopy images. (E) Western blots of signaling molecules in WT and *Panx3*$^{-/-}$ calvarial cells. The Panx3 ER Ca^{2+} channel promotes NFATc1 activity. Downregulation of activities of signaling molecules in the Panx3 ER-mediated NFATc1 pathway in *Panx3*$^{-/-}$ calvarial cells. Calvarial cells were prepared from newborn WT and *Panx3*$^{-/-}$ mice and phosphorylation levels (P-) of Akt, CaMKII, and NFATc1 were analyzed by western blotting.

proliferating cells; thrombospondin-2 (Tsp2, also known as THBS2), a marker of periosteum and osteoblasts (Tucker, 1993), and perlecan, which is used to identify cartilage (Arikawa-Hirasawa et al., 1999; Costell et al., 1999; Ishijima et al., 2012). We found that the Ki67 staining increased in the proliferative chondrocyte zone, periosteum, bone collar, and trabecular bone of *Panx3*$^{-/-}$ growth plates, compared to their WT counterparts (Fig. 5A). An 5-ethynyl-2'-deoxyuridine (EdU) incorporation analysis also showed increased cell proliferation in the growth plate of *Panx3*$^{-/-}$ mice (data not shown). In the calvaria, the number of Ki67-positive cells

Journal of Cell Science (2016) 129, 1018-1030 doi:10.1242/jcs.176883

was also increased in newborn *Panx3*$^{-/-}$ mice relative to WT (Fig. 5B), indicating increased proliferation of osteoprogenitor cells in the absence of Panx3. Wnt/β-catenin signaling is required for the proliferation of osteoprogenitor cells (Ishikawa et al., 2014; Kato et al., 2002). Therefore, we examined the expression of a target gene of β-catenin, *Axin2*, in the growth plate and calvaria of *Panx3*$^{-/-}$ mice that contained an *Axin2-lacZ* knock-in allele. The number of lacZ-positive cells increased in the periosteum, growth plate bone and calvaria of *Panx3*$^{-/-}$ mice as compared to WT mice (Fig. 5Ca,b), indicating that Wnt/β-catenin signaling was sustained in the *Panx3*$^{-/-}$ osteoprogenitor cells. The modulation of Wnt/β-catenin signaling agrees with the western blot analysis using differentiating WT primary calvarial cells in culture (Fig. S4D). These results reveal that Panx3 negatively regulates the proliferation of osteoprogenitor cells in WT mice by inhibiting Wnt/β-catenin signaling.

Panx3 is an upstream molecule of Cx43 in bone formation

We explored whether Panx3 and Cx43 play any distinct roles during bone formation. First, skeletal abnormalities of newborn *Cx43*$^{-/-}$ mice, *Panx3*$^{-/-}$ mice and double-null *Panx3*$^{-/-}$;*Cx43*$^{-/-}$ mice were analyzed and compared with those in WT mice (Fig. 6Aa). As previously described (Lecanda et al., 2000), the gross appearance of newborn *Cx43*$^{-/-}$ mice skeletons displayed no obvious

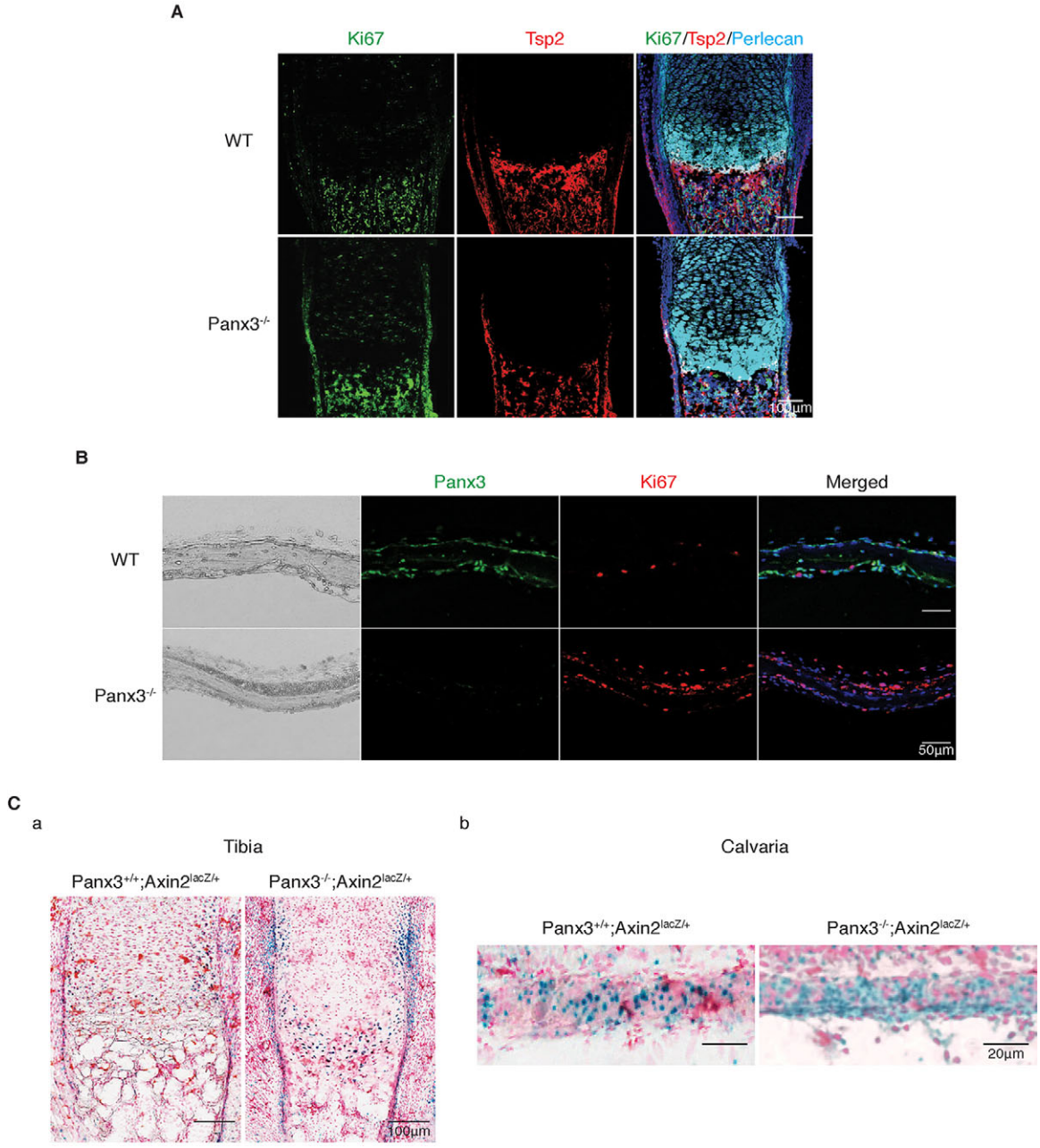

Fig. 5. *Panx3* knockout promotes osteoprogenitor cell proliferation. (A) Immunostaining the growth plates of the newborn mice with antibodies to Ki67 (green), Tsp2 (thrombospondin-2) (red) and perlecan (cyan). (B) Immunostaining calvaria of newborn mice with antibodies to Panx3 (green) and Ki67 (red). The nuclei were stained with Hoechst dye 33342 (blue). (C) *Panx3*$^{+/+}$;*Axin2*^{LacZ} (left panel) and *Panx3*$^{-/-}$;*Axin2*^{LacZ} (right panel) tibia (a) and calvaria (b) were stained with X-gal.

Journal of Cell Science (2016) 129, 1018-1030 doi:10.1242/jcs.176883

abnormalities except for a slightly smaller skull and less mineralization. The *Panx3*$^{-/-}$;*Cx43*$^{-/-}$ mice showed similar but slightly more severe skeletal abnormalities relative to *Panx3*$^{-/-}$ mice, such as shorter limbs and a smaller skull (Fig. 6Aa). A micro-computed tomography (μCT) analysis revealed that the density of many bones, such as the skull and the vertebral bones, was reduced in the newborn *Panx3*$^{-/-}$ mice in comparison to WT, and that the *Panx3*$^{-/-}$;*Cx43*$^{-/-}$ mice displayed more severe bone density defects. In contrast, the bone density of *Cx43*$^{-/-}$ mice was not significantly different from WT, the only exception being the skull (Fig. 6Ab,c; Movies 1–4).

The expression of Panx3 and Cx43 in the calvaria was compared between newborn WT, *Panx3*$^{-/-}$ and *Cx43*$^{-/-}$ mice by performing immunostaining (Fig. 6Ba). Cx43 expression was considerably reduced in *Panx3*$^{-/-}$ calvaria. However, Panx3 in *Cx43*$^{-/-}$ calvaria was expressed with levels that were almost identical to those observed in WT calvaria (Fig. 6Ba). In WT growth plates, Panx3 was expressed in the prehypertrophic zone, hypertrophic zone, periosteum, trabecular bone and bone collar, whereas Cx43 was expressed only in the periosteum and bone areas (Fig. 6Bb). Merged images of the double immunostaining clearly showed that both Panx3 and Cx43 were expressed in the bone areas, and that Panx3 (but not Cx43) was also expressed in cartilage (Fig. 6Bb). Similar to that of the calvaria, Cx43 expression was very much reduced in the growth plate of *Panx3*$^{-/-}$ mice (Fig. 6Bb). Timecourses of *Panx3* and *Cx43* mRNA expression patterns were analyzed during osteoblast differentiation of WT and *Cx43*$^{-/-}$ calvarial cells (Fig. 6Ca,b). We found that Panx3 was first induced at the early differentiation stage in WT cells. Interestingly, we observed that *Panx3* mRNA expression decreased at the mature osteoblast differentiation stage, concomitant with an increase in the *Cx43* mRNA expression levels (Fig. 6Ca). Similar *Panx3* expression patterns were also observed in *Cx43*$^{-/-}$ calvarial cells cultured in the osteoinduction medium (Fig. 6Cb).

We examined the mRNA expression levels of other marker genes for chondrocytes and osteoblasts by performing qPCR using mRNA from whole tibias of the three types of mutant mice used in our study (Fig. 6D,E). Compared to WT tibias, *Cx43*$^{-/-}$ tibias showed similar mRNA expression levels for *Col2a1*, *Agc1* and *Col10a1*, with slightly reduced levels of *Mmp13* (Fig. 6D). In contrast, the mRNA levels of *Col2a1* and *Agc1* in the *Panx3*$^{-/-}$ tibia were increased, whereas *Mmp13* mRNA levels were reduced (Figs 2C and 6D). In *Panx3*$^{-/-}$;*Cx43*$^{-/-}$ tibias, the expression levels of *Col2a1* and *Agc1* genes were further increased whereas *Mmp13* mRNA levels were further decreased relative to their *Panx3*$^{-/-}$ counterparts (Fig. 6D). The *Col10a1* and *Runx2* mRNA levels among the three mutant tibias were similar to WT levels (Fig. 6D). However, *Osx* and *Alp* mRNA levels were significantly reduced in the tibias of both *Panx3*$^{-/-}$ and *Panx3*$^{-/-}$;*Cx43*$^{-/-}$ mice, whereas these expression levels in *Cx43*$^{-/-}$ mice were similar to WT levels (Fig. 6E). *Osx* expression was also examined in *Cx43*$^{-/-}$;*Osx-GFP* mice. The number of Osx–GFP-positive cells was similar between *Cx43*$^{-/-}$ and WT tibias (Fig. 4D). We found that the overexpression of Osx increased Cx43 expression during osteogenic induction of C212 cells, and the inhibition of endogenous Osx by use of small interfering RNA (siRNA) against Osx reduced Cx43 expression (Fig. S4A). These results suggest that Panx3 promotes Cx43 expression by regulating Osx expression (see pathway in Fig. 8B). Although *Ocn* mRNA levels were decreased in *Cx43*$^{-/-}$ tibias and further decreased in *Panx3*$^{-/-}$ tibias, the *Ocn* mRNA levels were most reduced in the *Panx3*$^{-/-}$;*Cx43*$^{-/-}$ tibias (Fig. 6E).

Distinct functions of Panx3 and Cx43 in calvarial cell proliferation and differentiation

To further evaluate the functions of Panx3 and Cx43 in osteoblast proliferation and differentiation, we used primary calvarial cells prepared from the calvaria of newborn mutant mice, which contained osteoprogenitor cells. Expression of ALP (an early differentiation marker) and mineralization (a late differentiation process) were examined by immunostaining and Alizarin Red staining at 5 days and 16 days, respectively, after the cells were induced to differentiate in the osteoinduction medium. ALP expression in *Cx43*$^{-/-}$ calvarial cells was similar to WT, whereas mineralization was reduced (Fig. 7A). In contrast, both ALP expression and mineralization were reduced in *Panx3*$^{-/-}$ and *Panx3*$^{-/-}$;*Cx43*$^{-/-}$ calvarial cells (Fig. 7A). Next, we analyzed the cell proliferation of primary calvarial cells from the mutant mice. The proliferation of the *Panx3*$^{-/-}$ and *Panx3*$^{-/-}$;*Cx43*$^{-/-}$ calvarial cells increased compared to WT, whereas the proliferation of *Cx43*$^{-/-}$ and WT cells were similar (Fig. 7B). These results suggest that Panx3 plays a role in the cell cycle exit and the transition stage from cell proliferation to differentiation, whereas Cx43 is not involved in the transition stage.

To further confirm the functions of Panx3 and Cx43 in osteoblast differentiation, we performed rescue experiments by transfection of *Panx3*$^{-/-}$ calvarial cells with an expression vector for Panx3, Osx or Cx43. ALP expression was restored in the *Panx3*$^{-/-}$ cells by transfection with either the Panx3 or the Osx vector, whereas Cx43 transfection was unable to rescue ALP expression (Fig. 7Ca). Panx3, but not Cx43, transfection also restored the mRNA expression levels of both Osx and Ocn (Fig. S4B). We also examined whether Panx3 overexpression rescues the mineralization defect in *Panx3*$^{-/-}$ and *Cx43*$^{-/-}$ primary calvarial cells after infection of the adenovirus Panx3 expression vector Ad-Panx3 (Fig. 7Cb). The mineralization defect in the *Panx3*$^{-/-}$ cells was rescued by the Ad-Panx3 infection. Ad-Panx3 infection into the *Cx43*$^{-/-}$ cells was also able to rescue the mineralization defect. These results indicate that Panx3 can replace Cx43 functions, but Cx43 cannot replace Panx3 functions.

It is known that Panx3 has functions as a hemichannel, a gap junction and an ER Ca^{2+} channel (Ishikawa et al., 2011). We examined these activities in primary calvarial cells from mutant mice. We first examined the ER Ca^{2+} channel activity in calvarial cells of mutant mice (Fig. 7Da). No significant difference was found in the level of the Ca^{2+} released from the ER to the cytosol induced by ATP between WT and *Cx43*$^{-/-}$ cells; in contrast, the ER Ca^{2+} channel activity in *Panx3*$^{-/-}$ cells was reduced. The reduction level in ER Ca^{2+} channel activity in *Panx3*$^{-/-}$;*Cx43*$^{-/-}$ cells was similar to that in *Panx3*$^{-/-}$ cells. Hemichannel activity was studied in mutant calvarial cells by measuring intracellular ATP release into the extracellular space (Fig. 7Db). The hemichannel activity in *Cx43*$^{-/-}$ cells was slightly reduced compared to WT, and *Panx3*$^{-/-}$ cells displayed a significant reduction in hemichannel activity; however, the *Panx3*$^{-/-}$;*Cx43*$^{-/-}$ cells showed the most severe reduction in hemichannel activity. We observed similar reduction patterns in the hemichannel activities of all mutant calvarial cells when the channel was activated by cell membrane depolarization resulting from potassium gluconate (KGlu) treatment. We measured gap junction activity in primary calvarial cells from mutant mice by analyzing Ca^{2+} wave propagation. In the assay, the cells were loaded with a photosensitive caged Ca^{2+} and Ca^{2+}-sensitive Fluo-4. The Ca^{2+} wave propagation was initiated from a single cell through illumination by a two-photon laser, then analyzed with live-cell fluorescence confocal microscopy (Fig. 7Dc; Fig. S4C; Movies 5–16). Gap junction activity in the *Cx43*$^{-/-}$ cells was

Journal of Cell Science (2016) 129, 1018-1030 doi:10.1242/jcs.176883

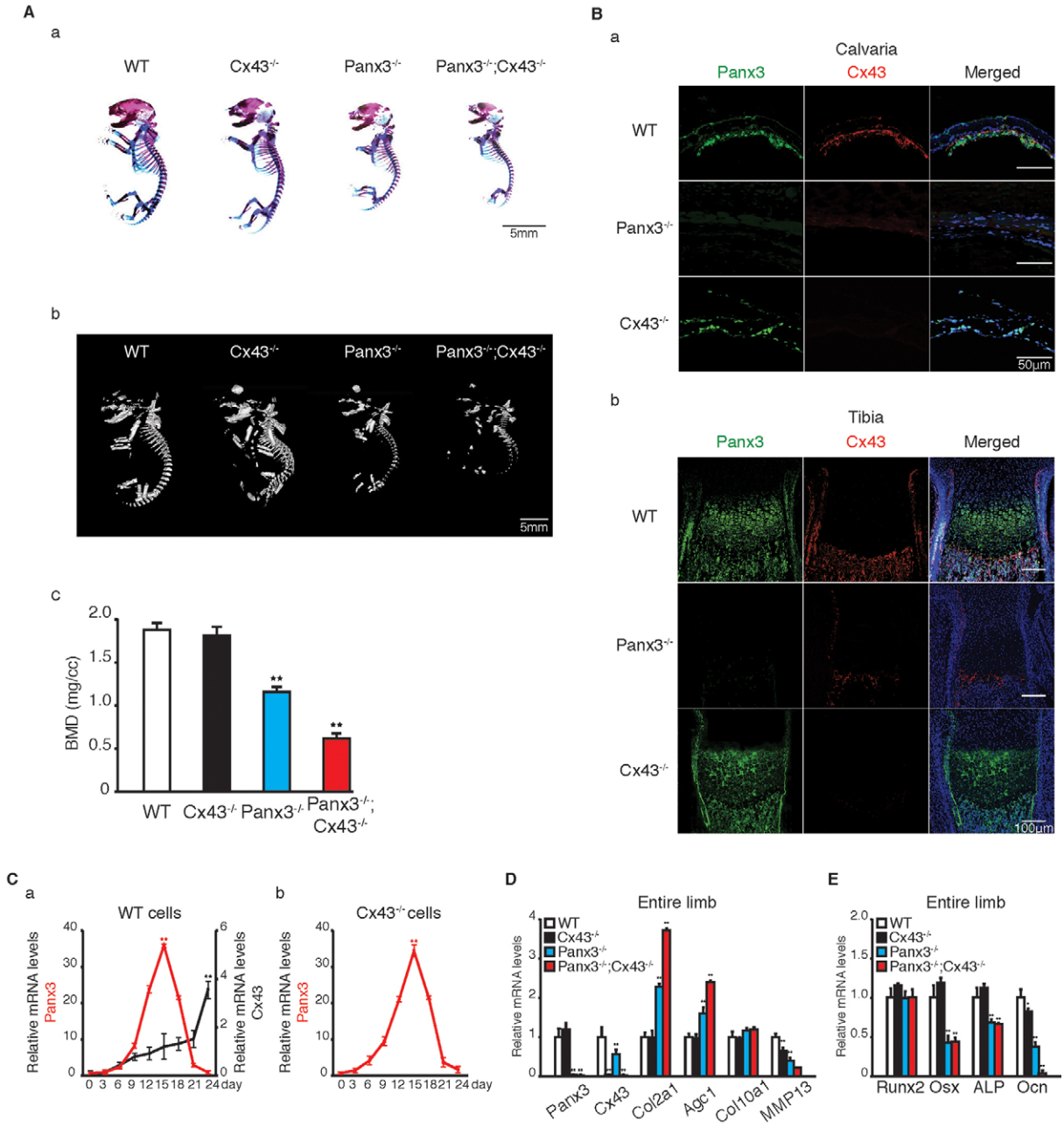

Fig. 6. Panx3 is upstream of Cx43 in osteoblast differentiation. (A) (a) Alizarin Red and Alcian Blue staining of the whole skeletons of newborn WT, *Cx43*$^{-/-}$, *Panx3*$^{-/-}$ and *Panx3*$^{-/-}$;*Cx43*$^{-/-}$ mice. (b) μCT analysis of WT, *Cx43*$^{-/-}$, *Panx3*$^{-/-}$ and *Panx3*$^{-/-}$;*Cx43*$^{-/-}$ bones. (c) Quantification of bone mineral density (BMD). (B) Immunostaining. (a) The newborn calvarias (a) and growth plates of the tibias (b) were stained with antibodies to Panx3 (green) and Cx43 (red). The nuclei were stained with Hoechst dye 33342 (blue). (C) qPCR analyses of *Panx3* and *Cx43* mRNA expression during osteoblast differentiation in primary calvarial cells from WT (a) and *Cx43*$^{-/-}$ mice (b). Primary calvarial cells were cultured in the osteogenic induction medium. Total RNA was extracted from the cells at the indicated days after the osteogenic induction. (D) qPCR analysis of the mRNA expression of the chondrogenic marker genes and the *Panx3* and *Cx43* genes using RNA isolated from the whole tibias of newborn WT, *Cx43*$^{-/-}$, *Panx3*$^{-/-}$ and *Panx3*$^{-/-}$;*Cx43*$^{-/-}$ mice. (E) qPCR analysis of the mRNA expression of osteogenic marker genes using RNA isolated from the whole tibias of newborn WT, *Cx43*$^{-/-}$, *Panx3*$^{-/-}$, and *Panx3*$^{-/-}$;*Cx43*$^{-/-}$ mice. Results represent the mean±s.d., *n*=3. **P*<0.05, ***P*<0.01 [Student's *t*-test (Ca,Cb) and one-way ANOVA (Ac,D,E)].

reduced compared with WT, whereas the reduction in *Panx3*$^{-/-}$ cells was even more profound; however, *Panx3*$^{-/-}$;*Cx43*$^{-/-}$ cells showed the most severe reduction. We found that carbenoxolone (CBX), a gap junction inhibitor, but not Apyrase, an ATP receptor antagonist, inhibited Ca^{2+} wave propagation (Fig. S4C). These results suggest that Ca^{2+} wave propagation is mediated through gap junctions, not ATP receptors. Taken together, our results reveal that Panx3 functions in all three channel activities, whereas Cx43 functions as a hemichannel and a gap junction, but not as an ER Ca^{2+} channel.

DISCUSSION

In this study, we demonstrate that Panx3 regulates growth plate development and bone formation, having functions and expression patterns in chondrogenesis and osteogenesis that are distinct from Cx43. Panx3 deficiency reduced the expression of multiple

Journal of Cell Science (2016) 129, 1018-1030 doi:10.1242/jcs.176883

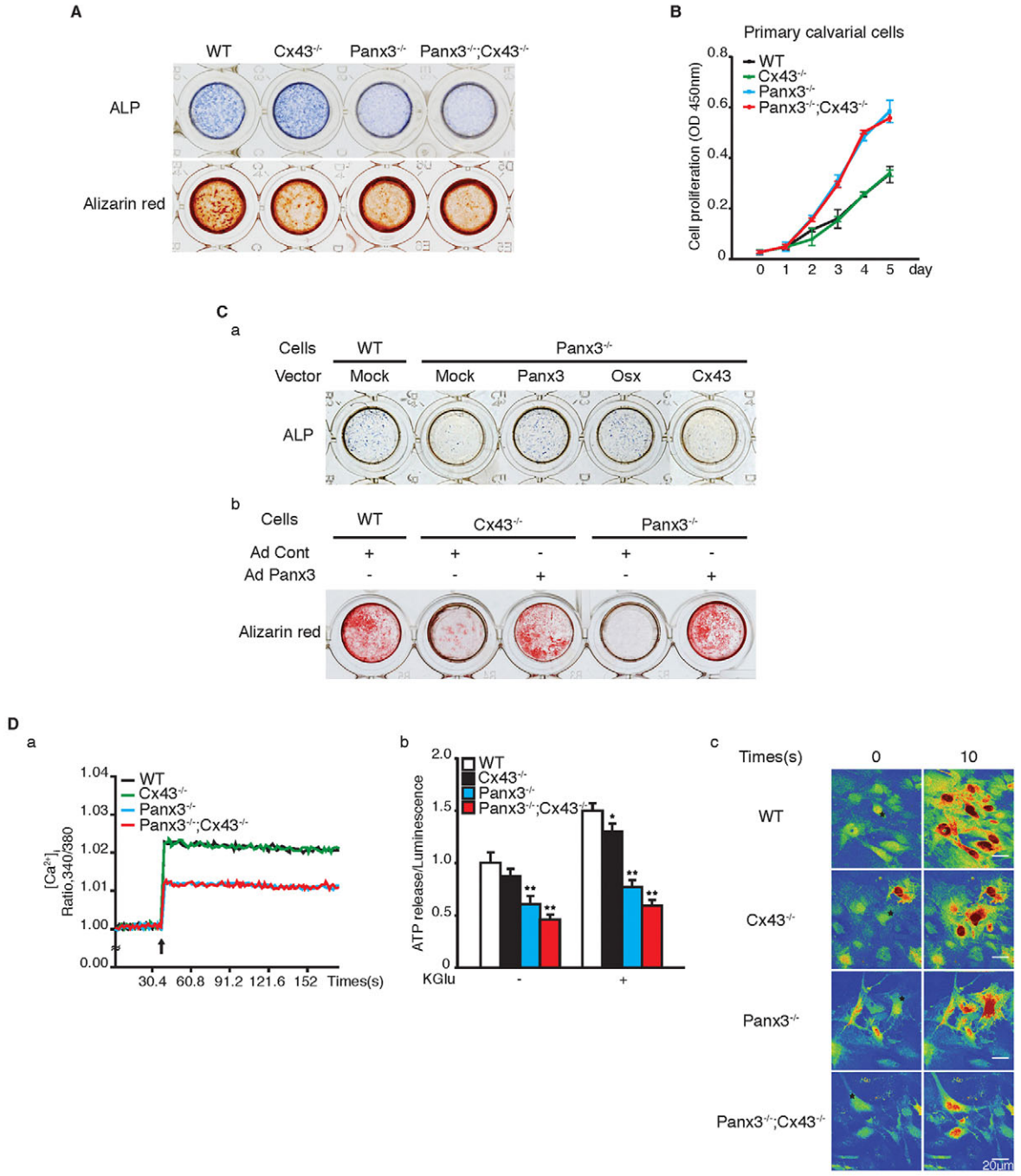

Fig. 7. Panx3 plays a role that is distinct from Cx43 during osteogenesis. (A) Representative ALP staining (top) and Alizarin Red S staining (bottom) of primary calvarial cells isolated from newborn WT, *Cx43*$^{-/-}$, *Panx3*$^{-/-}$, and *Panx3*$^{-/-}$;*Cx43*$^{-/-}$ mice. For the ALP staining, cells were cultured in osteoinduction media for 5 days; 16 days for the Alizarin Red S staining. (B) Proliferation of primary calvarial cells isolated from newborn WT (black), *Cx43*$^{-/-}$ (green), *Panx3*$^{-/-}$ (blue), and *Panx3*$^{-/-}$;*Cx43*$^{-/-}$ (red) mice. The cells were cultured in proliferation media (α-MEM), and the proliferation was measured at the indicated days after the culture. (C) (a) Rescues of osteoblast differentiation defects of primary *Panx3*$^{-/-}$ calvarial cells by transfection of an expression vector for Mock, Panx3, Osx or Cx43. Representative ALP staining of *Panx3*$^{-/-}$ calvarial cells at 3 days after transfection. (b) Rescues of the osteoblast differentiation defects of primary *Cx43*$^{-/-}$ and *Panx3*$^{-/-}$ calvarial cells by infection of control adenovirus (Ad Cont) or Panx3-adenovirus (Ad Panx3). Representative Alizarin Red S staining of the cells at 16 days after infection. (D) Channel activities of primary calvarial cells from newborn WT, *Cx43*$^{-/-}$, *Panx3*$^{-/-}$ and *Panx3*$^{-/-}$;*Cx43*$^{-/-}$ mice. (a) ER Ca^{2+} channel activities. The increase in intracellular Ca^{2+} released from the ER by ATP stimulation (arrow) was measured. The data shown are representative of at least three different experiments. (b) Hemichannel activities. ATP release into the extracellular space was measured with and without KGlu for 2 min. (c) Gap junction activities. Caged Ca^{2+} was uncaged within a single cell by laser illumination; Ca^{2+} wave propagation was measured at 10 s after the illumination. The data shown are representative of at least three different experiments. Results represent the mean±s.d., *n*=3. **P*<0.05, ***P*<0.01 (one-way ANOVA).

osteoblast differentiation markers, including early markers *Osx* and *ALP*, and a late marker *Ocn*. We found that forced Panx3 expression in *Panx3*$^{-/-}$ primary calvarial cells restored these expression levels (Fig. 7Ca; Fig. S4B), suggesting that Panx3 promotes the early and late stages of osteoblast differentiation by regulating *Osx* expression. Panx3 activates the signaling pathway from Akt to

Journal of Cell Science (2016) 129, 1018-1030 doi:10.1242/jcs.176883

Panx3, the ER Ca^{2+} channel, CaM CaMKII and, finally, calcineurin (Ishikawa et al., 2011). Active calcineurin dephosphorylates phosphorylated NFATc1 and converts it into active NFATc1, which activates *Osx* expression. Osx expression subsequently induces downstream osteoblast genes, such as *Alp* and *Ocn* (Koga et al., 2005; Nakashima et al., 2002). We demonstrated that activities of these signaling molecules were downregulated in *Panx3*$^{-/-}$ calvarial cells (Fig. 4E). It is known that Runx2 is upstream of Osx, as it is the earliest osteoblast differentiation marker. In contrast to *Osx* expression, there was no observable difference in *Runx2* levels between the WT and *Panx3*$^{-/-}$ limb (Fig. 6E). It has been reported that Runx2 binds to the *Panx3* promoter and increases the reporter activity in DNA transfection assays (Bond et al., 2011). These results suggest that Runx2 is upstream of Panx3 and regulates Panx3 expression.

The sizes of skeletal elements of P1 *Cx43*$^{-/-}$ mice were similar to those of WT mice, with the only exceptions being a slightly smaller skull and less mineralization (Fig. 6Aa); these results are consistent with previous observations (Lecanda et al., 2000). Contrary to their Cx43$^{-/-}$ counterparts, all of the skeletal elements of *Panx3*$^{-/-}$ mice were short with reduced mineralization. Double-knockout *Panx3*$^{-/-}$;*Cx43*$^{-/-}$ mice displayed skeletal abnormalities similar to those of *Panx3*$^{-/-}$ mice, but with more severe phenotypes. We found that the differences in expression patterns and functional activities between Panx3 and Cx43 were attributable to the skeletal abnormalities of these mutant mice. The limb abnormalities observed in *Panx3*$^{-/-}$ mice, but not *Cx43*$^{-/-}$ mice, are likely due to a requirement for Panx3 to be expressed in chondrocytes, whereas Cx43 does not appear necessary (Fig. 6Bb).

The expression patterns of Panx3 and Cx43 were also different during osteoblast differentiation by WT primary calvarial cells. *Panx3* mRNA was induced at the early differentiation stage, whereas its expression levels decreased at the late differentiation stage. The expression pattern of Cx43 was opposite to that of Panx3 – *Cx43* mRNA expression increased at the late stage, despite being relatively low during the early stage. In addition, Cx43 expression was downregulated in both the *Panx3*$^{-/-}$ calvaria and growth plate. Mineralization was reduced in all three types of mutant mice and calvarial cells. These results suggest that Panx3 is required for both the early and late differentiation of osteoblasts, whereas Cx43 is involved primarily at the late stage of differentiation. This supposition is further supported by the failure of forced Cx43 expression to restore osteoblast gene expression levels and mineralization in *Panx3*$^{-/-}$ calvarial cells. In contrast, forced Panx3 expression in *Cx43*$^{-/-}$ cells was able to rescue the defect in mineralization. Thus, Panx3 is upstream of Cx43 and regulates Cx43 expression in part by promoting Osx expression. In normal late osteoblast differentiation, Panx3 levels decrease whereas Cx43 levels are upregulated, allowing Cx43 to play a role in mineralization.

Differentiation of osteoclasts was reduced in the growth plates and in the calvaria of *Panx3*$^{-/-}$ mice. Given that Panx3 was not expressed during osteoclast differentiation, this reduction is due to impaired osteoblast differentiation in Panx3$^{-/-}$ mice. In contrast, Cx43 is expressed during osteoclast differentiation and likely directly regulates osteoclast differentiation. Regardless of whether the mechanism is indirect or direct, both Panx3 and Cx43 regulate osteoclast differentiation and play roles in both bone formation and homeostasis.

Panx3 functions as a hemichannel, an ER Ca^{2+} channel, and a gap junction (Ishikawa et al., 2011). Although all of these Panx3 activities are involved in the promotion of cell cycle exit and subsequent osteoblast differentiation, the hemichannel is the first to be involved in these processes. This was demonstrated previously by adding inhibitors specific to Panx3 hemichannel activity in cultures, which resulted in the elimination of Panx3 ER Ca^{2+} channel and gap junction activities, as well as the inhibition of cell cycle exit and differentiation of osteoblasts (Ishikawa et al., 2011). The Panx3 ER Ca^{2+} channel, which releases Ca^{2+} from the ER into the cytosol through ATP receptor–PI3K–Akt signaling, is crucial for osteoblast differentiation (Ishikawa et al., 2011). Both Panx3 and Cx43 display gap junction and hemichannel functions. However, we found that Cx43 lacks ER Ca^{2+} channel activity, marking another important difference between Cx43 and Panx3 (Fig. 7Da). The lack of the ER Ca^{2+} channel function of Cx43 might explain why forced Cx43 expression is unable to induce Osx and other differentiation genes in *Paxn3*$^{-/-}$ calvarial cells.

Canonical Wnt signaling is involved in bone formation by promoting proliferation of osteoprogenitor cells and mineralization (Almeida et al., 2005; Kato et al., 2002). BMP2 promotes osteoblast differentiation by inducing the Runx2 and Osx transcription factors, which subsequently induce downstream osteoblast marker genes. Panx3 is also induced in WT calvaria cells by BMP2 (Fig. 6C; Fig. S4B). Taken together, our results suggest a new cascade pathway of BMP2–Runx2–Panx3–Osx in osteoblast differentiation. During the normal late differentiation stage, the expression of *Panx3* mRNA and protein is downregulated, whereas the expression of Cx43 is upregulated (Fig. 6C). During the early differentiation stage, the level of active β-catenin was decreased and that of phosphorylated β-catenin was increased, suggesting reduced Wnt/β-catenin signaling (Fig. S4D). We also found that phosphorylated β-catenin was decreased and active β-catenin was increased at the late differentiation stage, concomitant with a reduction in Panx3 expression, suggesting increased Wnt/β-catenin signaling (Fig. S4D). Given that Wnt signaling is required for mineralization during the late differentiation stage, our results suggest an upregulation of Wnt/β-catenin signaling, which is consistent with a previous report that Cx43 expression is induced by Wnt signaling (van der Heyden et al., 1998). Osx was also found to regulate Cx43 expression (Fig. S4B), but the mechanism of Panx3 downregulation at the late differentiation stage is not yet clear. Some *in vivo* evidence suggests that Runx2 is suppressed at the maturation stage at both the transcriptional and functional levels (Hesse et al., 2010). Therefore, it is possible that Panx3 expression is downregulated because of the reduced Runx2 activity at the late differentiation stage.

We provide evidence that Panx3 regulates skeletal formation through mechanisms that are distinct from those employed by Cx43. Our results demonstrate that Panx3 regulates bone formation by modulating Wnt/β-catenin signaling and regulating Osx and Cx43 expression. In addition, Panx3 promotes differentiation of mature chondrocytes and vascular invasion in cartilage. Thus, Panx3 exerts multiple functions in the cascades of endochondral and intramembranous ossification (Fig. 8).

MATERIALS AND METHODS

Mouse lines

For construction of the *Panx3*-targeting vector, a 10-kb Eco*R1* genomic fragment containing exons 1 from bac clone RPCI22-47H21 (Invitrogen) was used for gene targeting (Fig. S1). The targeting vector (PMK3) was linearized by SacII digestion and electroporated into W4 embryonic stem cells. One targeted clone produced chimeric mice that transmitted the mutated allele through the germ line. Heterozygous *Panx3*$^{+/-}$ mice were generated, with at least five generations, by backcrossing to C57BL/6 mice. We analyzed phenotypes of *Panx3*$^{-/-}$ mice after five or six generations of backcrossing. Heterozygous *Cx43*$^{+/-}$ (Huang et al., 1998), *Axin2*$^{lacZ/+}$

Journal of Cell Science (2016) 129, 1018-1030 doi:10.1242/jcs.176883

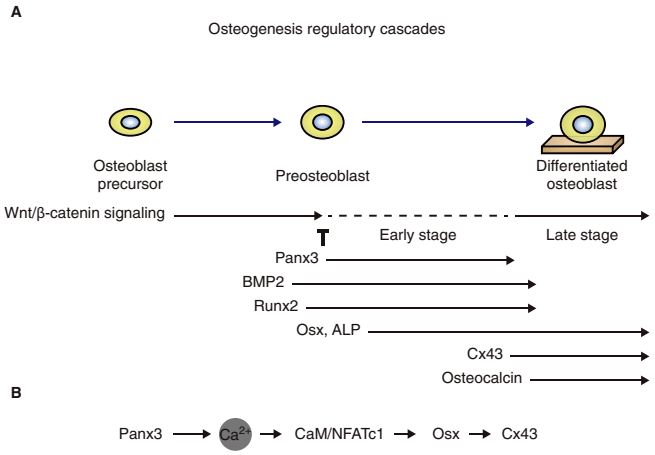

Fig. 8. The appearance of Panx3 and Cx43 relative to other molecules in the cascades of osteoblast differentiation. (A) Panx3 is induced in the transition stage from proliferation to differentiation by BMP2 and Runx2, and promotes cell cycle exit by inhibiting Wnt/β-catenin signaling through its hemichannel. Panx3 also promotes the expression of differentiation marker genes such as Osx and ALP by activating NFAT through the ER Ca^{2+} channel, CaMKII and calcineurin pathway. At the maturation stage, Panx3 is downregulated and Cx43 is upregulated, concomitant with increased Wnt/β-catenin signaling and decreased BMP2 signaling. (B) Panx3-mediated CaM and NFATc1 signaling increases Osx expression, which promotes Cx43 transcription.

(Lustig et al., 2002), and *Osx-GFP Cre/+* mice (Rodda and McMahon, 2006) were obtained from the Jackson Laboratory (stock numbers 2908839, 009120 and 006361, respectively). The animal protocol approved by the NIDCR Animal Care and Use Committee was used for maintaining and handling mice. All animals were housed in an animal facility approved by the American Association for the Accreditation of Laboratory Animal Care.

Reagents

Rabbit anti-Panx3 antibody was used as previously described (Ishikawa et al., 2011; Iwamoto et al., 2010). Control adenovirus (AdCont) and Panx3 expression adenovirus (AdPanx3) were prepared and purified by Welgen Inc. The antibodies against OPN (1:100 dilution, catalog number AF808) and ALP (1:100 dilution, catalog number AF2910) were obtained from R&D Systems, Inc.; MMP13 (1:100 dilution, catalog number ab39012) and Osx (1:100 dilution, catalog number ab22552) from Abcam; CD31 (1:100 dilution, catalog number 553370) and Tsp2 (1:100 dilution, catalog number 611150) from BD Biosciences; VEGF (1:100 dilution, catalog number sc-507) from Santa Cruz Biotechnology; Cx43 (immunostaining, 1:100 dilution; western blotting, 1:500 dilution; catalog number C7857-05) from US Biological; Ocn (1:100 dilution, catalog number BT-592) from Biomedical Technology; phosphorylated β-catenin (1:500 dilution, catalog number 9561), phosphorylated GSK3β (1:500 dilution, catalog number 5558) and GSK3 (1:500 dilution, catalog number 12456) from Cell Signaling Technology, Inc.; β-catenin (1:500 dilution, catalog number C7082) and α-tubulin (1:1000 dilution, catalog number T9026) from Sigma; Ki67 from Dako, and active β-catenin (1:500 dilution, catalog number 05-665) from Millipore. BMP2 was obtained from HumanZyme, and iQ SYBR Green Supermix from BioRad. Horseradish peroxidase (HRP)-conjugated goat anti-mouse-IgG and goat anti-rabbit-IgG antibodies were obtained from US Biological. siOsx was obtained from Thermo. CBX and Apyrase were from Sigma-Aldrich. The inhibitory Panx3 peptide and its control scrambled peptide were used as previously described (Ishikawa et al., 2011; Iwamoto et al., 2010).

Cell culture

Primary calvarial cells were prepared from calvaria of newborn mice and cultured in α-minimum essential medium (α-MEM, Invitrogen) with 10% fetal bovine serum (FBS), as previously described (Matsunobu et al., 2009). For osteoblast differentiation, the cells were cultured in osteoinduction medium, including 50 μg/ml ascorbic acid and 5 mM β-glycerophosphate. For the rescue experiments, primary calvarial cells were isolated from WT, $Cx43^{-/-}$ or $Panx3^{-/-}$ mice. The $Panx3^{-/-}$ calvarial cells were transfected with an expression vector for Panx3 (pEF1/Panx3), Osx (pCA1F-Osx), Cx43 (pEF1/Cx43) or control empty vector (pEF1), and cultured in the osteoinduction medium for 3 days for ALP staining. For mineralization assays, the $Panx3^{-/-}$ and $Cx43^{-/-}$ calvarial cells were infected with AdPanx3 or AdCont (1×10^9 pfu/ml) virus and cultured in the osteoinduction medium for 16 days; the medium was changed and more virus was added every 3 days. For the proliferation assay, primary calvarial cells isolated were cultured for up to 5 days. The cell proliferation activity was measured using a Cell Counting Kit-8 (Dojindo) following the manufacturer's instruction.

Skeletal preparation and μCT

Newborn WT, $Cx43^{-/-}$, $Panx3^{-/-}$ and $Panx3^{-/-}$;$Cx43^{-/-}$ mice were processed for skeletal preparations using a standard Alcian Blue and Alizarin Red staining protocol (Matsunobu et al., 2009). For the μCT analysis, whole bodies of newborn WT, $Panx3^{-/-}$, $Cx43^{-/-}$ and $Panx3^{-/-}$; $Cx43^{-/-}$ mice were scanned using the μCT scanner (μCT 50, SCANCO Medical AG). The 3D images were constructed and analyzed with the evaluation software of the μCT system.

Direct GFP fluorescence, X-gal staining and immunostaining

For direct GFP fluorescence observation and X-gal staining, tibias and calvarial samples from newborn mice were embedded in an OCT compound (Tissue-Tek) without fixation for cryosectioning; X-gal staining was performed as previously described (Kopp et al., 2007). For immunostaining, the tissues of the newborn mice were fixed in paraformaldehyde overnight, embedded in paraffin, and cut into 10-μm sections. The sections were treated with heat-induced epitope retrieval in pH 6.0 citrate buffer (Dako). Primary antibodies were detected with Alexa Fluor 488- (Invitrogen), Cy-3- (Jackson ImmunoResearch Laboratories) or Cy-5-conjugated secondary antibodies as previously described (Ishikawa et al., 2011). Nuclear staining was performed with Hoechst 33342 dye (Sigma-Aldrich). Analysis was performed on an LSM 710 inverted confocal microscope (Carl Zeiss MicroImaging, Inc.).

In situ hybridization

In situ hybridization was performed as described previously (Iwamoto et al., 2010). Briefly, digoxigenin-11-UTP-labeled, single-stranded antisense RNA probes for *Ihh* were prepared using the DIG RNA labeling kit (Roche Applied Science). Frozen tissue sections from P1 growth plates were used for *in situ* hybridization.

RT-PCR

Total RNA (1 μg) was used for PCRs with gene-specific primers (Table S1) as previously described (Iwamoto et al., 2010). qPCR was performed with iQ SYBR Green Supermix (Bio-Rad) and Eco Real-time PCR System (Illumina). qPCR was performed for 40 cycles, at 95°C for 15 s, and at 60°C for 1 min. Gene expression levels were normalized to those of the housekeeping gene *Hprt*.

ATP flux

The ATP flux was determined by luminometry, as previously described (Ishikawa et al., 2011; Iwamoto et al., 2010). Primary calvarial cells were seeded at 1.0×10^4 cells/well in a 96-well plate, and cultured for 1 day with α-MEM containing 10% FBS. The cells were then washed with PBS, followed by incubation in PBS with or without KGlu solution (140 mM KGlu, 10 mM KCl, and 5.0 mM TES, pH 7.5) for 2 min. The supernatant was collected and assayed with luciferase and luciferin (Promega). The luminescence was measured using a Mithras LB 940 multimode plate reader (Berthold).

Measurement of $[Ca^{2+}]_i$ and imaging of Ca^{2+} wave propagation

Measurement of $[Ca^{2+}]_i$ and imaging of Ca^{2+} wave propagation were examined as previously described (Ishikawa et al., 2011). To measure $[Ca^{2+}]_i$, primary calvarial cells were cultured in a 96-well plate

for 3 days and then loaded with 5 µM Fura-2AM (Invitrogen) in HBSS for 45 min at 37°C in 5% CO_2. For analyses of Ca^{2+} wave propagation, primary calvarial cells seeded in a glass-bottomed dish were incubated in HBSS containing 4 µM of the Ca^{2+} indicator Fluo-4 AM, 10 µM pluronic F-127 (Invitrogen), 0.1% OxyFluor (Oxyrase), and 2.5 µM caged reagent NP-EGTA AM (Invitrogen) for 30 min at room temperature, followed by washing and incubation with Ca^{2+}-free HBSS. To block the gap junction channels, the cells were incubated with 25 µM CBX. To inhibit ATP receptors, the cells were incubated with 20 U Apyrase. Caged Ca^{2+} was uncaged by illuminating a single cell with a two-photon laser set at 730 nm; Ca^{2+} wave propagation was measured at 10 s after the illumination.

Western blot analysis

Protein samples were prepared from cell lysates, electrophoresed on 4–12% SDS-polyacrylamide gels, transferred onto membranes and blotted with antibodies as previously described (Iwamoto et al., 2010).

Data analysis

Each experiment was repeated several times and the data was analyzed using Prism 5 software. Student's *t*-tests were used to highlight differences between two groups of data. One-way ANOVA was used for the quantification of BMD (Fig. 6Ac), qPCR (Fig. 6D,E; Fig.S4B) and ATP release (Fig. 7Db). $P<0.05$ was considered statistically significant.

Acknowledgements

We thank Azusa Maeda and Marian Young for their valuable suggestions, and Hynda Kleinman, Kenneth Yamada, and Ellika Salari for critical reading.

Competing interests

The authors declare no competing or financial interests.

Author contributions

M.I. and Y.Y. designed the experiments. M.I., G.L.W., T.I., K.S. and S.F. performed the experiments. M.I. and Y.Y. wrote the manuscript with input from all other co-authors.

Funding

This work was supported in part by the Intramural Research Program of the National Institute of Dental and Craniofacial Research, USA [grant number DE000483-24, -25, and-26 to Y.Y.]; Grants-in-Aid from the Ministry of Education, Science, and Culture of Japan [grant number 26670880 to S.F.]; and the NEXT program [grant number LS010 to S.F.]. M.I. and T.I. were supported in part by the Research Fellowship of the Japan Society for the Promotion of Science for Young Scientists. Deposited in PMC for release after 12 months.

Supplementary information

Supplementary information available online at
http://jcs.biologists.org/lookup/suppl/doi:10.1242/jcs.176883/-/DC1

References

Almeida, M., Han, L., Bellido, T., Manolagas, S. C. and Kousteni, S. (2005). Wnt proteins prevent apoptosis of both uncommitted osteoblast progenitors and differentiated osteoblasts by beta-catenin-dependent and -independent signaling cascades involving Src/ERK and phosphatidylinositol 3-kinase/AKT. *J. Biol. Chem.* **280**, 41342-41351.

Arikawa-Hirasawa, E., Watanabe, H., Takami, H., Hassell, J. R. and Yamada, Y. (1999). Perlecan is essential for cartilage and cephalic development. *Nat. Genet.* **23**, 354-358.

Baranova, A., Ivanov, D., Petrash, N., Pestova, A., Skoblov, M., Kelmanson, I., Shagin, D., Nazarenko, S., Geraymovych, E., Litvin, O. et al. (2004). The mammalian pannexin family is homologous to the invertebrate innexin gap junction proteins. *Genomics* **83**, 706-716.

Barbe, M. T., Monyer, H. and Bruzzone, R. (2006). Cell-cell communication beyond connexins: the pannexin channels. *Physiology* **21**, 103-114.

Berridge, M. J., Lipp, P. and Bootman, M. D. (2000). The versatility and universality of calcium signalling. *Nat. Rev. Mol. Cell Biol.* **1**, 11-21.

Bond, S. R., Lau, A., Penuela, S., Sampaio, A. V., Underhill, T. M., Laird, D. W. and Naus, C. C. (2011). Pannexin 3 is a novel target for Runx2, expressed by osteoblasts and mature growth plate chondrocytes. *J. Bone Miner. Res.* **26**, 2911-2922.

Chung, D. J., Castro, C. H. M., Watkins, M., Stains, J. P., Chung, M. Y., Szejnfeld, V. L., Willecke, K., Theis, M. and Civitelli, R. (2006). Low peak bone mass and attenuated anabolic response to parathyroid hormone in mice with an osteoblast-specific deletion of connexin43. *J. Cell Sci.* **119**, 4187-4198.

Civitelli, R. (2008). Cell–cell communication in the osteoblast/osteocyte lineage. *Arch. Biochem. Biophys.* **473**, 188-192.

Costell, M., Gustafsson, E., Aszódi, A., Mörgelin, M., Bloch, W., Hunziker, E., Addicks, K., Timpl, R. and Fässler, R. (1999). Perlecan maintains the integrity of cartilage and some basement membranes. *J. Cell Biol.* **147**, 1109-1122.

D'Hondt, C., Ponsaerts, R., De Smedt, H., Bultynck, G. and Himpens, B. (2009). Pannexins, distant relatives of the connexin family with specific cellular functions? *Bioessays* **31**, 953-974.

Giepmans, B. N. (2004). Gap junctions and connexin-interacting proteins. *Cardiovasc. Res.* **62**, 233-245.

Hervé, J.-C. and Derangeon, M. (2013). Gap-junction-mediated cell-to-cell communication. *Cell Tissue Res.* **352**, 21-31.

Hesse, E., Saito, H., Kiviranta, R., Correa, D., Yamana, K., Neff, L., Toben, D., Duda, G., Atfi, A., Geoffroy, V. et al. (2010). Zfp521 controls bone mass by HDAC3-dependent attenuation of Runx2 activity. *J. Cell Biol.* **191**, 1271-1283.

Huang, G. Y., Cooper, E. S., Waldo, K., Kirby, M. L., Gilula, N. B. and Lo, C. W. (1998). Gap junction-mediated cell-cell communication modulates mouse neural crest migration. *J. Cell Biol.* **143**, 1725-1734.

Ishijima, M., Suzuki, N., Hozumi, K., Matsunobu, T., Kosaki, K., Kaneko, H., Hassell, J. R., Arikawa-Hirasawa, E. and Yamada, Y. (2012). Perlecan modulates VEGF signaling and is essential for vascularization in endochondral bone formation. *Matrix Biol.* **31**, 234-245.

Ishikawa, M., Iwamoto, T., Nakamura, T., Doyle, A., Fukumoto, S. and Yamada, Y. (2011). Pannexin 3 functions as an ER Ca(2+) channel, hemichannel, and gap junction to promote osteoblast differentiation. *J. Cell Biol.* **193**, 1257-1274.

Ishikawa, M., Iwamoto, T., Fukumoto, S. and Yamada, Y. (2014). Pannexin 3 inhibits proliferation of osteoprogenitor cells by regulating Wnt and p21 signaling. *J. Biol. Chem.* **289**, 2839-2851.

Iwamoto, T., Nakamura, T., Doyle, A., Ishikawa, M., de Vega, S., Fukumoto, S. and Yamada, Y. (2010). Pannexin 3 regulates intracellular ATP/cAMP levels and promotes chondrocyte differentiation. *J. Biol. Chem.* **285**, 18948-18958.

Karsenty, G. and Wagner, E. F. (2002). Reaching a genetic and molecular understanding of skeletal development. *Dev. Cell* **2**, 389-406.

Kato, M., Patel, M. S., Levasseur, R., Lobov, I., Chang, B. H.-J., Glass, D. A., II, Hartmann, C., Li, L., Hwang, T.-H., Brayton, C. F. et al. (2002). Cbfa1-independent decrease in osteoblast proliferation, osteopenia, and persistent embryonic eye vascularization in mice deficient in Lrp5, a Wnt coreceptor. *J. Cell Biol.* **157**, 303-314.

Koga, T., Matsui, Y., Asagiri, M., Kodama, T., de Crombrugghe, B., Nakashima, K. and Takayanagi, H. (2005). NFAT and Osterix cooperatively regulate bone formation. *Nat. Med.* **11**, 880-885.

Kopp, H. G., Hooper, A. T., Shmelkov, S. V. and Rafii, S. (2007). Beta-galactosidase staining on bone marrow. The osteoclast pitfall. *Histol. Histopathol.* **22**, 971-976.

Kronenberg, H. M. (2003). Developmental regulation of the growth plate. *Nature* **423**, 332-336.

Lecanda, F., Warlow, P. M., Sheikh, S., Furlan, F., Steinberg, T. H. and Civitelli, R. (2000). Connexin43 deficiency causes delayed ossification, craniofacial abnormalities, and osteoblast dysfunction. *J. Cell Biol.* **151**, 931-944.

Lustig, B., Jerchow, B., Sachs, M., Weiler, S., Pietsch, T., Karsten, U., van de Wetering, M., Clevers, H., Schlag, P. M., Birchmeier, W. et al. (2002). Negative feedback loop of Wnt signaling through upregulation of conductin/axin2 in colorectal and liver tumors. *Mol. Cell. Biol.* **22**, 1184-1193.

Matsunobu, T., Torigoe, K., Ishikawa, M., de Vega, S., Kulkarni, A. B., Iwamoto, Y. and Yamada, Y. (2009). Critical roles of the TGF-beta type I receptor ALK5 in perichondrial formation and function, cartilage integrity, and osteoblast differentiation during growth plate development. *Dev. Biol.* **332**, 325-338.

Nakashima, K., Zhou, X., Kunkel, G., Zhang, Z., Deng, J. M., Behringer, R. R. and de Crombrugghe, B. (2002). The novel zinc finger-containing transcription factor osterix is required for osteoblast differentiation and bone formation. *Cell* **108**, 17-29.

Paznekas, W. A., Boyadjiev, S. A., Shapiro, R. E., Daniels, O., Wollnik, B., Keegan, C. E., Innis, J. W., Dinulos, M. B., Christian, C., Hannibal, M. C. et al. (2003). Connexin 43 (GJA1) mutations cause the pleiotropic phenotype of oculodentodigital dysplasia. *Am. J. Hum. Genet.* **72**, 408-418.

Plotkin, L. I., Lezcano, V., Thostenson, J., Weinstein, R. S., Manolagas, S. C. and Bellido, T. (2008). Connexin 43 is required for the anti-apoptotic effect of bisphosphonates on osteocytes and osteoblasts in vivo. *J. Bone Miner. Res.* **23**, 1712-1721.

Reaume, A. G., de Sousa, P. A., Kulkarni, S., Langille, B. L., Zhu, D., Davies, T. C., Juneja, S. C., Kidder, G. M. and Rossant, J. (1995). Cardiac malformation in neonatal mice lacking connexin43. *Science* **267**, 1831-1834.

Rodda, S. J. and McMahon, A. P. (2006). Distinct roles for Hedgehog and canonical Wnt signaling in specification, differentiation and maintenance of osteoblast progenitors. *Development* **133**, 3231-3244.

Seo, J. H., Jin, Y.-H., Jeong, H. M., Kim, Y.-J., Jeong, H. G., Yeo, C.-Y. and Lee, K.-Y. (2009). Calmodulin-dependent kinase II regulates Dlx5 during osteoblast differentiation. *Biochem. Biophys. Res. Commun.* **384**, 100-104.

Söhl, G. and Willecke, K. (2004). Gap junctions and the connexin protein family. *Cardiovasc. Res.* **62**, 228-232.

Journal of Cell Science (2016) 129, 1018-1030 doi:10.1242/jcs.176883

Tucker, R. P. (1993). The in situ localization of tenascin splice variants and thrombospondin 2 mRNA in the avian embryo. *Development* **117**, 347-358.

van der Heyden, M. A., Rook, M. B., Hermans, M. M., Rijksen, G., Boonstra, J., Defize, L. H. and Destree, O. H. (1998). Identification of connexin43 as a functional target for Wnt signalling. *J. Cell Sci.* **111**, 1741-1749.

Vanden Abeele, F., Bidaux, G., Gordienko, D., Beck, B., Panchin, Y. V., Baranova, A. V., Ivanov, D. V., Skryma, R. and Prevarskaya, N. (2006). Functional implications of calcium permeability of the channel formed by pannexin 1. *J. Cell Biol.* **174**, 535-546.

Watkins, M., Grimston, S. K., Norris, J. Y., Guillotin, B., Shaw, A., Beniash, E. and Civitelli, R. (2011). Osteoblast connexin43 modulates skeletal architecture by regulating both arms of bone remodeling. *Mol. Biol. Cell* **22**, 1240-1251.

Zayzafoon, M. (2006). Calcium/calmodulin signaling controls osteoblast growth and differentiation. *J. Cell Biochem.* **97**, 56-70.

Zelzer, E., McLean, W., Ng, Y. S., Fukai, N., Reginato, A. M., Lovejoy, S., D'Amore, P. A. and Olsen, B. R. (2002). Skeletal defects in VEGF(120/120) mice reveal multiple roles for VEGF in skeletogenesis. *Development* **129**, 1893-1904.